Oscillatory burst discharge generated through conditional backpropagation of dendritic spikes

Ray W. Turner[a],*, Neal Lemon[a], Brent Doiron[b], Asim J. Rashid[c],
Ezequiel Morales[a], Andre Longtin[b], Leonard Maler[d], Robert J. Dunn[c]

[a]Neuroscience Research Group, University of Calgary, Calgary Alberta, Canada T2N 4N1
[b]Physics Department, University of Ottawa, Ontario, Canada K1N 6N5
[c]Center for Research in Neuroscience, Montreal General Hospital, Montreal PQ, Canada H3G 1A4
[d]Department of Cellular and Molecular Medicine, University of Ottawa, Ottawa Ontario, Canada K1H 8M5

Abstract

Gamma frequencies of burst discharge (>40 Hz) have become recognized in select cortical and non-cortical regions as being important in feature extraction, neural synchrony and oscillatory discharge. Pyramidal cells of the electrosensory lateral line lobe (ELL) of *Apteronotus leptorhynchus* generate burst discharge in relation to specific features of sensory input in vivo that resemble those recognized as gamma frequency discharge when examined in vitro. We have shown that these bursts are generated by an entirely novel mechanism termed conditional backpropagation that involves an intermittent failure of dendritic Na^+ spike conduction. Conditional backpropagation arises from a frequency-dependent broadening of dendritic spikes during repetitive discharge, and a mismatch between the refractory periods of somatic and dendritic spikes. A high threshold class of K^+ channel, *Apt*Kv3.3, is expressed at high levels and distributed over the entire soma-dendritic axis of pyramidal cells. *Apt*Kv3.3 channels are shown to contribute to the repolarization of both somatic and dendritic spikes, with pharmacological blockade of dendritic Kv3 channels revealing an important role in controlling the threshold for burst discharge. The entire process of conditional backpropagation and burst output is successfully simulated using a new compartmental model of pyramidal cells that incorporates a cumulative inactivation of dendritic K^+ channels during repetitive discharge. This work is important in demonstrating how the success of spike backpropagation can control the output of a principle sensory neuron, and how this process is regulated by the distribution and properties of voltage-dependent K^+ channels.
© 2003 Elsevier Ltd. All rights reserved.

Keywords: Dendritic spike; Burst discharge; Electrosensory; DAP; Compartmental model

1. Introduction

Oscillatory discharge is a widespread form of neuronal output that has been linked to a variety of neural functions, including sensory processing, rhythmic motor output, and the synchronization of cell populations that underlie oscillatory discharge associated with different states of consciousness [26,54,59]. Oscillatory discharge in cortical neurons has often been defined as the rhythmic discharge of single spikes at rates up to and including gamma frequencies (>40 Hz) [40,41]. The generation of an oscillatory series of spike *bursts* has typically been associated with thalamo-cortical networks, within a frequency range of 0.1 to ~20 Hz

[35,58]. The mechanisms underlying burst discharge in this range are well understood, and include both synaptic and ionic factors. More recently select cortical and subcortical neurons have been found capable of generating oscillatory burst discharge with a period that occurs at even the highest gamma frequencies. Cells that exhibit this activity have been dubbed as chattering cells, high threshold bursters, or fast rhythmic bursters, although all share similarities in burst discharge characteristics [8,9,18,27,52,57,59]. The mechanisms underlying burst output at these high frequencies have only recently come under investigation [8,62,63,68].

We recently identified the mechanism underlying gamma frequency burst discharge in a pyramidal cell of the electrosensory lateral line lobe (ELL) of the weakly electric fish *Apteronotus leptorhynchus* (Brown Ghost Knife fish) [13,25,63]. The highly laminar organization of

---

the ELL provides ready access to somatic and dendritic regions of pyramidal cells in in vitro slice preparations, allowing us to identify key elements that underlie or modulate burst discharge. This work has shown that ELL pyramidal cells employ an entirely novel mechanism for generating burst output that arises from differences in the properties of somatic and dendritic Na^+ spikes. These differences produce an intermittent failure of spike backpropagation from the soma into apical dendrites that groups repetitive discharge into a series of spike bursts [13,25]. The simplicity of the mechanisms underlying this "conditional backpropagation" makes it very likely that it will be used in many other bursting neurons. The importance of this work was further emphasized by the finding that ELL pyramidal cells generate burst discharge *in vivo* in relation to specific aspects of sensory input, indicating a role for spike bursts in at least feature extraction [15,37]. The generation of burst discharge is also apparently under the control of descending synaptic inputs in vivo [2,3], providing a means of regulating burst discharge in relation to ongoing sensory information.

This review will briefly summarize the features that regulate dendritic spike backpropagation in ELL pyramidal cells, as examined through in vitro slice and dissociated cell preparations, and through use of a recently constructed compartmental model.

2. Materials and methods

All recordings of spike discharge were obtained using a well established in vitro ELL slice preparation and single microelectrode recordings from either the soma or apical dendrites of separate pyramidal cells [25,63]. Synaptic inputs were activated by placement of a bipolar nichrome stimulating electrode on the tractus stratum fibrosum (tSF). Outside-out patch clamp recordings of *Apt*Kv3.3 K^+ channels were obtained using a spread-print preparation that provides an organotypic and partially dissociated thin ELL tissue slice maintained in vitro [46]. All recordings were obtained at room temperature. Average values are expressed as mean ± S.D. and statistical significance calculated using a Wilcoxon Signed Ranks test or student's *T*-test (**$P < 0.05$; ***$P < 0.001$). The model was generated from a reconstructed basilar pyramidal cell as 312 compartments of varying diameter and length using the simulation software *Neuron*, with ion channel distributions and spike properties constrained as much as possible by experimental data [13]. All further details as to dissection procedures, molecular and immunocytochemical protocols, and kinetic parameters used in the compartmental model can be found in recent publications [13,25,45,46].

3. Results

3.1. ELL structure and physiology

The ELL is a medullary nucleus that is in direct receipt of primary afferent input from ganglion cells that transmit the activity of electroreceptors on the body surface. The ELL is highly laminar in being comprised of a dorsal molecular layer, pyramidal cell layer, granule cell layer and a ventral deep fiber layer containing primary afferent inputs [5,32]. It is further organized into four distinct sensory maps of electroreceptor distribution that can be visualized in transverse sections across the medio-lateral extent as a medial (MS), centromedial (CMS), centrolateral (CLS) and lateral (LS) segment (Fig. 1A) [5]. The three more lateral maps (CMS, CLS, LS) receive a common input from tuberous electroreceptors that trifurcate before terminating on the basilar dendrites of granule or pyramidal cells. Anatomical work indicates no substantial difference in the underlying circuitry or any connections between these maps [32,34]. Despite these similarities in circuitry and afferent input, recordings in vivo have revealed a differential sensitivity of pyramidal cells across the CMS, CLS and LS maps to the frequency of sensory input. Shumway [55] first reported a difference in pyramidal cell responsiveness to the frequency of amplitude modulations of an externally applied electric field, with CMS cells responding best to low frequencies (∼1–10 Hz) and LS to higher frequencies (∼50–120 Hz) [55]. Distinctions between these maps were later made at the functional level by their required presence for such behaviours as the Jamming Avoidance Response (CMS) or detecting transient variations in the electric organ discharge (chirps) used for communication purposes (LS) [36]. These results indicate the presence of a neural mechanism that is regulated across the sensory maps to establish pyramidal cell frequency sensitivity.

Our work using in vitro ELL slice preparations has identified two forms of oscillatory discharge that could act as postsynaptic mechanisms to establish pyramidal cell responsiveness to sensory input. One is a relatively slow form of oscillatory discharge that is generated by slow subthreshold shifts in membrane potential that drives repetitive spike discharge in pyramidal cells [65]. This form of oscillation also exhibits identifiable shifts in such factors as oscillation period, burst duration, and spike frequency across the sensory maps that are consistent with the frequency sensitivity of pyramidal cells in vivo. Our preliminary data strongly suggests that this slow form of oscillation is driven by ELL granule cells, with pyramidal cell discharge following the rhythmic activity of granule cells through gap junction and synaptic connections (R.W. Turner, L. Maler, unpublished observations).

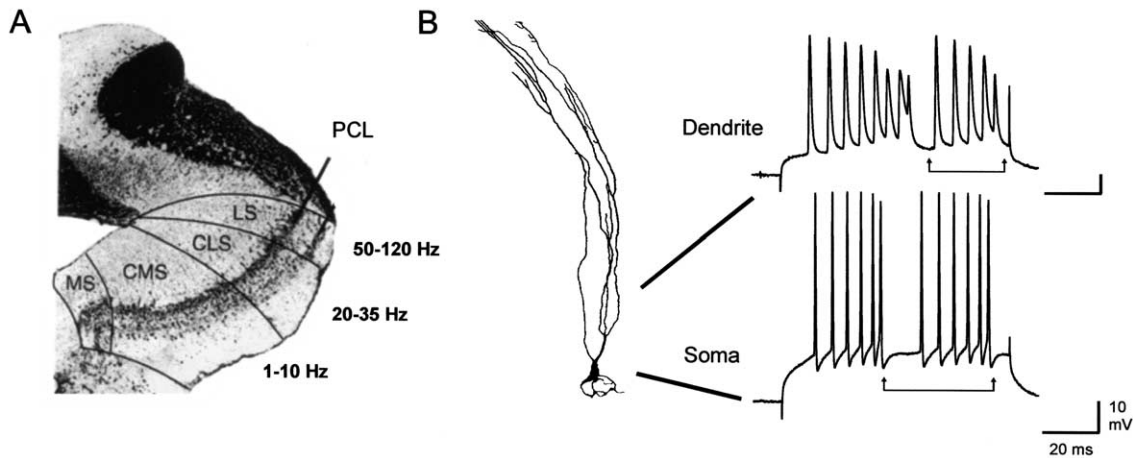A second form of oscillation arises entirely from an interaction between somatic and dendritic regions of

Fig. 1. ELL structure and physiology. (A) A transverse cresyl-violet stained section at the level of the medulla illustrating the laminar organization of the ELL, with a prominent pyramidal cell layer (PCL) containing the cell bodies of pyramidal cells. Lines indicate the boundaries between four separate topographic maps in which pyramidal cells in the outside three maps (CMS, CLS, LS) have been shown to differentially respond to the frequency of amplitude modulations in an applied external electric field (*insets* beside ELL maps) [55]. (B) Biocytin-filled pyramidal cell and representative recordings of current-evoked burst discharge in separate CMS pyramidal cell impalements at the level of the soma or proximal apical dendrites in vitro. Note that spike bursts are composed of a sequence of spikes that increase in frequency and are terminated by a spike doublet and burst AHP (burst AHPs and oscillation period are denoted by linked *arrows*).

pyramidal cells that gives rise to a process termed "conditional backpropagation" [25]. This process results in a repeating series of spike bursts that are entirely intrinsic to pyramidal cells and can be recorded at both the somatic and proximal apical dendritic level (Fig. 1B). Given the similarities between this form of burst discharge and the spike bursts recorded in vivo, this review will focus on the soma–dendritic interactions that underlie conditional backpropagation. Work discussed in this review also pertains almost exclusively to pyramidal cells positioned in the CMS sensory map when examined in vitro at room temperature.

3.2. Pyramidal cell spike discharge and afterpotentials

Like other central neurons examined to date, the lowest threshold for Na^+ spike discharge in ELL pyramidal cells is in the soma/axon hillock region, ensuring that depolarizations will initiate spike discharge near the soma [63]. ELL pyramidal cells are also similar to many other cell types in expressing a sufficient density of Na^+ channels in apical dendrites to support an active backpropagation of Na^+ spikes from the soma. Pyramidal cells differ from most other cells, however, in that these spikes conduct actively over only ∼200 μm of a ∼800 μm dendritic tree. As a result, there are characteristic differences in somatic and dendritic spikes, and these differences increase rapidly with distance from the soma [61]. Somatic spikes are large in amplitude and narrow in duration, and are followed by both fast and slow afterhyperpolarizations (fAHP, sAHP). By comparison, dendritic spikes are smaller in amplitude, rapidly increase in duration with distance from the soma, and are followed by only a sAHP (Fig. 2A). We determined

that the large difference in the duration of somatic and dendritic spikes provides a situation in which dendritic spikes promote return current flow to the soma to generate a depolarizing afterpotential (DAP) (Fig. 2B). The somatic DAP proves to be a very important aspect of membrane excitability, in that during repetitive spike discharge the amplitude of the DAP is potentiated (Fig. 2C). As a result, the AHPs that follow somatic spikes decrease in their ability to repolarize the cell, allowing the DAP to steadily increase the frequency of spike discharge. Eventually the DAP triggers a high frequency doublet at the soma that is followed by a large amplitude burst AHP that temporarily inhibits spike discharge (Fig. 2C). A similar pattern of spike discharge occurs in the dendrites, although the spike doublet and burst AHP are reduced in amplitude compared to the soma (Fig. 2C). This pattern of activity is produced in a repeating manner to group spike output into a oscillatory series of spike bursts. It is a pattern of output that proves to be very characteristic and reproducible, and generated in at least 60% of both basilar and non-basilar pyramidal cell classes in the CMS [25].

3.3. Factors underlying oscillatory burst discharge

Given the clear influence of the DAP in pyramidal cells, we have examined the soma–dendritic interactions that regulate DAP amplitude. This work indicates that DAP potentiation during repetitive discharge does not involve a progressive decrease in the amplitude of the somatic fAHP or sAHP (i.e. through a shift in E_K), or any recurrent Ca^{2+}-dependent synaptic connections [25]. We also have no evidence for a contribution by the hyperpolarization-activated inward currents I_h or I_T to
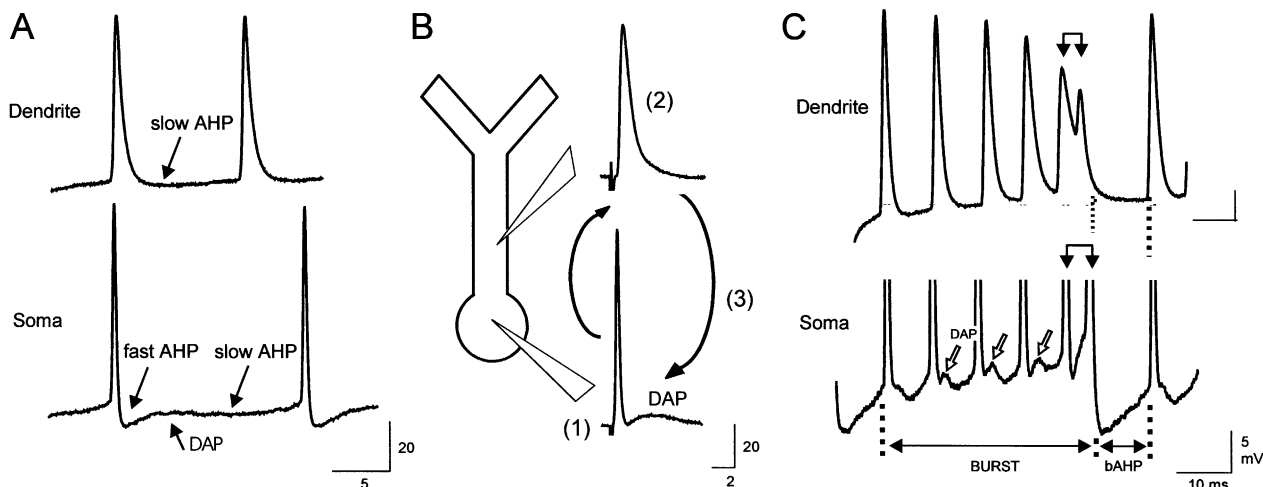
Fig. 2. Soma–dendritic interactions in spike discharge drive the burst depolarization. (A) Representative dendritic and somatic spike recordings from separate pyramidal cells illustrating differences in spike duration and afterpotentials. (B) Hypothesis for the generation of a somatic DAP, in which spike discharge initiated at the soma (1) backpropagates and increases in duration over the proximal apical dendrites (2). The longer duration dendritic spike re-depolarizes the soma as a DAP (3). (C) Expanded view of a single spike burst in separate somatic and dendritic recordings aligned for comparison. The somatic DAP is potentiated during repetitive spike discharge until it generates a high frequency somatic spike doublet (double linked *arrows*). The doublet is followed by a burst AHP (*bAHP*) that terminates a given burst and promotes recovery from changes in dendritic and somatic potentials. Spike amplitude in the somatic recording in C are truncated.

burst discharge in CMS pyramidal cells. Comparisons between somatic and dendritic spike discharge, however, have revealed key differences that promote DAP potentiation. The first is that during current-evoked burst discharge, there is a selective increase in the duration of dendritic (but not somatic) spikes (Fig. 3A and B). This results primarily from a decrease in the rate of repolarization of dendritic spikes (Fig. 3A–C), with a concomitant decrease in the amplitude of the dendritic sAHP, and an increase in dendritic spike duration of up to 60% over control by even the third spike of a burst (Fig. 3A and C) [25].

A second aspect of burst discharge is the existence of a clear threshold for generating burst output. During the presentation of low levels of current injection, pyramidal cells exhibit only tonic spike discharge, but undergo a transition to burst output as current injection is increased. A current-frequency analysis revealed that burst threshold is characterized by the occurrence of interspike intervals (ISIs) in the range of $\sim$3–8 ms ($\sim$125–300 Hz; Fig. 3D) [25]. By controlling the ISI between spike discharge using antidromic stimulus pairs, we determined that ISIs in this range evoked not only an increase in dendritic spike duration, but also a temporal summation of dendritic spikes that increased the net membrane voltage in the apical dendrite (Fig. 3E). This range of ISIs corresponds closely to those that promote a potentiation of the DAP at the soma (Fig. 3F).

The close correspondence between dendritic voltage and DAP amplitude in the antidromic condition-test experiments extended even to a decrease in both parameters at ISIs shorter than $\sim$3 ms (Fig. 3E and F). A

decrease in DAP amplitude at short ISIs was previously proposed to reflect a failure or reduction of dendritic spike discharge at ISIs that approached the dendritic spike refractory period [63]. Indeed, the third important factor for burst discharge is a gradual increase in the relative refractory period of spike discharge from the soma and over the proximal apical dendrites (Fig. 4) [25]. The reason for an increase in refractory period has not been firmly established, but likely relates to a decrease in the density of both Na^+ channels and K^+ channels involved in spike repolarization with distance along the dendritic tree. The final difference in refractory period between somatic and distal dendrites is substantial, in that spikes recorded only $\sim$200 μm from the soma can exhibit a refractory period over three times longer than that in somatic recordings (Fig. 4B). On average, we found that the relative refractory period at the soma was 2.6 ± 0.64 ms ($n = 12$), while that in dendritic recordings $\geqslant 100$ μm from the soma was 4.5 ± 0.93 ms ($n = 14$). By comparison, the average ISI for spike doublets measured at the soma was 3.9 ± 1.08 ms ($n = 12$), indicating that the ISI of spike doublets fall within the dendritic refractory period.

3.4. Conditional backpropagation

The three factors identified above proved to be sufficient to account for the generation of burst discharge in pyramidal cells, as summarized in Fig. 5. Our working hypothesis is that during repetitive discharge at ISIs above $\sim$8 ms, spike discharge initiated at the soma is faithfully backpropagated into apical dendrites (Fig. 5A). At ISIs less than $\sim$8 ms, repetitive discharge
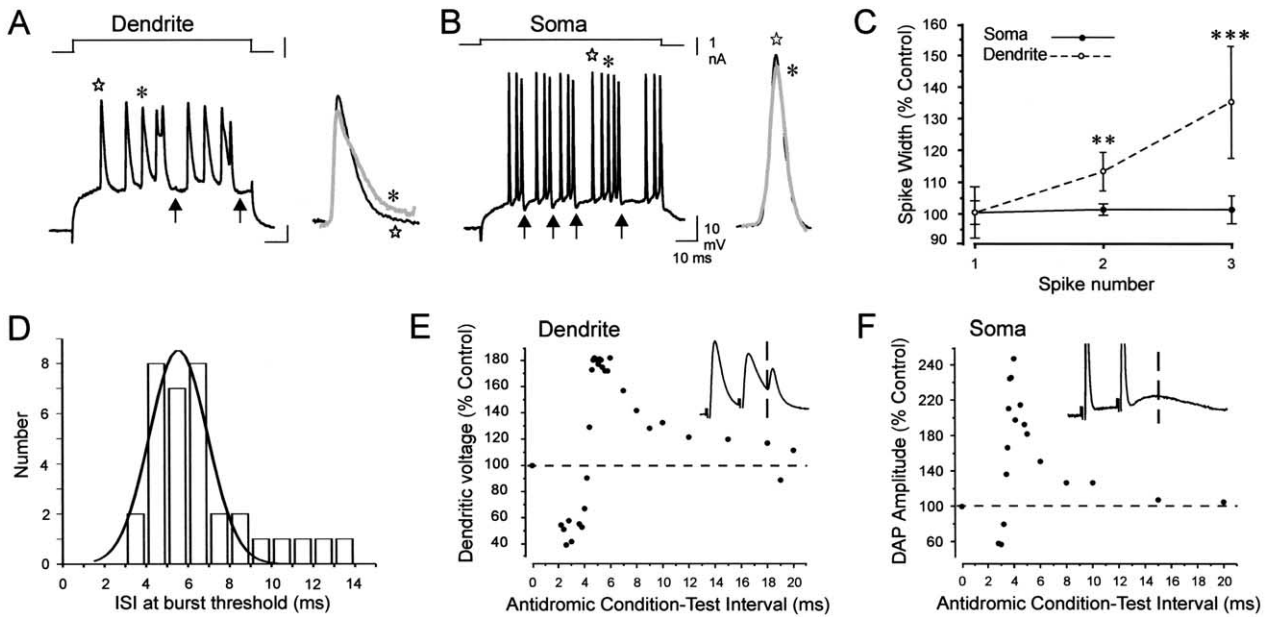
Fig. 3. Frequency-dependent control of spike and burst discharge properties. (A) A dendritic recording of two current-evoked bursts (burst AHPs denoted by *arrows*). *Inset* at right shows expanded and superimposed views of the first (*dark trace*) and third dendritic spike (*grey trace*) in the indicated burst. Note the substantial decrease in the rate of repolarization and increase in dendritic spike duration during a burst. (B) A separate somatic recording exhibiting spike bursts in response to current injection. Note the lack of change in the rate of somatic spike repolarization during a burst (*inset*). (C) Plot of the average spike width for the recordings shown in A and B (excluding spike doublets). Note the select change in dendritic spike properties ($n = 7$ somatic and 8 dendritic bursts). Spike width was measured at a time corresponding to 10% of spike amplitude. (D) An interval histogram of the average ISI at the threshold for current-evoked burst discharge indicates that burst discharge begins at ISIs between ~ 3 and 8 ms ($n = 32$ soma and 11 dendrites; binwidth = 1). Data were fit by a Gaussian function to a peak value of 5.5 ± 1.38 ms. (E) and (F) Plots of the absolute voltage of the dendritic response and somatic DAP at varying antidromic condition–test (C–T) intervals in two representative cases. *Insets* provide examples of spike pairs at C-T intervals of 4.7 ms (E) and 3.7 ms (F). Dashed lines indicate the latency for measurement of voltage at the estimated peak of the somatic DAP. Note the close correspondence between the absolute voltage attained in apical dendrites and somatic DAP amplitude, including a gradual reduction at shorter C–T intervals. Data are modified from [25] with permission from Journal of Neurophysiology.

promotes a frequency-dependent broadening of dendritic spikes that potentiates the somatic DAP (Fig. 5B). The DAP eventually triggers a spike doublet that is outside the range of the somatic spike refractory period, allowing two full somatic spikes to be discharged (Fig. 5B). However, the ISI of spike doublets is *inside* the refractory period of dendritic membrane. As a result, the first spike of the somatic doublet backpropagates, but the second fails to conduct, leading to one full dendritic spike and a small potential as the second component of the dendritic spike doublet. This small potential proves to be very similar to the response previously established as representing a passive reflection of spike discharge at the soma. The generation of a spike doublet thus signifies the functional equivalent of "shutting down" the entire dendritic depolarization from one spike to the next, allowing the membrane to repolarize in the form of a burst AHP. The burst AHP provides sufficient time for recovery from the changes induced during the previous spike burst, allowing this sequence of events to be repeated.

The above process in which dendritic spikes first drive burst discharge in a frequency-dependent manner, but then exceed a limit defined by their refractory period to block backpropagation represents an entirely novel

mechanism for generating burst discharge. We view this as an inherently simple and highly reproducible endpoint that results from basic differences in the properties of somatic and dendritic spikes. Yet it is very dynamic in generating burst discharge at frequencies that range from 5–150 Hz; the widest range of burst output that we are aware of in a central neuron. Our most recent work indicates that this range of burst frequencies is closely linked to the rate of potentiation of the DAP [39]. Since the rate of DAP potentiation reflects activity in dendrites, we have examined K^+ channels in pyramidal cells that could account for the change in dendritic spike repolarization.

3.5. Dendritic K^+ channels and burst discharge

Voltage-dependent ion channels are known to be distributed widely over the soma–dendritic axis of neurons, with important consequences to the properties of spike discharge in dendritic regions [19,29,30,56,64,71]. The "Kv3" (*Shaw*) class of K^+ channels have many characteristics that make them well suited to control the rate of spike repolarization. Each of the four principle subtypes defined in mammals (Kv3.1–Kv3.4) share the properties of a high threshold for activation (~ -10
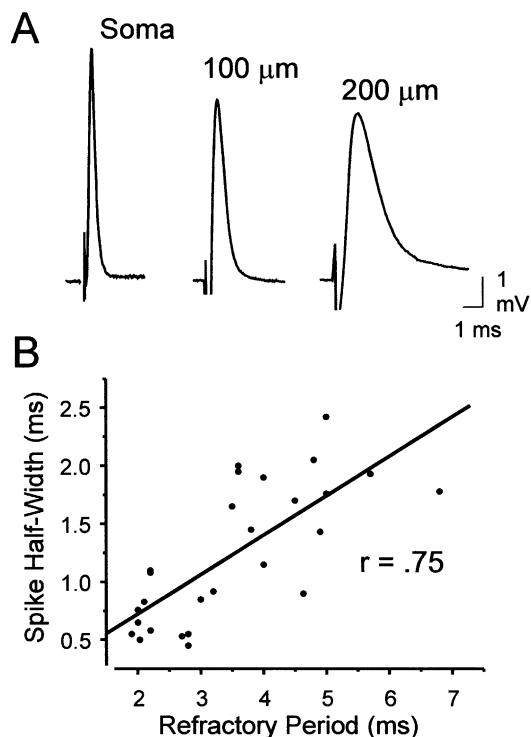
Fig. 4. Spike refractory period increases over the soma-dendritic axis. (A) Representative examples of antidromically evoked spike discharge in separate somatic and dendritic recordings at ∼100 μm and 200 μm from the soma. Note the decrease in spike amplitude and increase in duration with distance from the soma. (B) A scatter plot of relative refractory periods measured with antidromic stimulus pairs at all locations with respect to spike half-width indicates a substantial increase in refractory period with distance from the soma ($n = 27$; $r = 0.75$; $P < 0.0001$). Data are modified from [25] with permission from Journal of Neurophysiology.
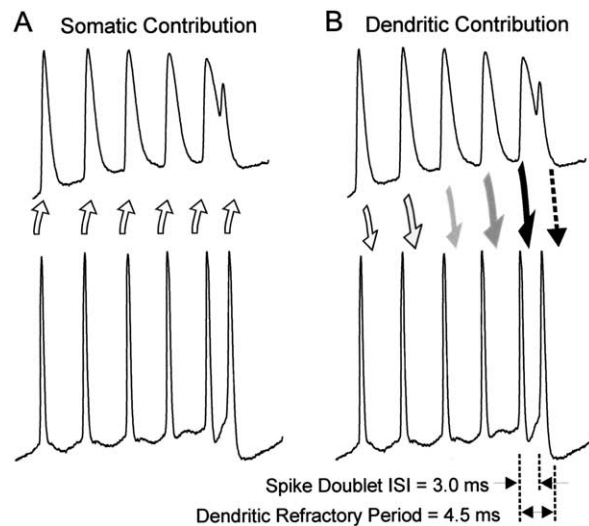

Fig. 5. Working hypothesis of conditional backpropagation. (A) and (B) Representative spike bursts in separate pyramidal cell somatic and dendritic recordings aligned for comparison. The records in A illustrate the somatic contribution to dendritic activity during a burst, while records in B the dendritic contribution to the somatic burst depolarization. The relative weights of influence are shown by the size and shading of arrows. (A) Each successive somatic spike during the early phase of a burst triggers a full backpropagating dendritic spike. (B) Beyond a minimal spike frequency of ∼125 Hz, successive dendritic spikes in a burst are longer in duration than the last, progressively increasing current flow back to the soma (shaded *arrows*). There is a resulting potentiation of DAP amplitude until the DAP reaches threshold to trigger a spike doublet at the soma. The refractory period of dendritic membrane (4.5 ms) is longer than the ISI of the spike doublet (3.0 ms), which prevents backpropagation of the second spike of the pair. This failure of backpropagation eliminates the dendritic depolarization that drives the spike burst (denoted by *dashed arrow*), and is followed by membrane repolarization by a subsequent burst AHP. Data are taken from [25] with permission from Journal of Neurophysiology.

mV) and a fast rate of activation and deactivation [49]. As such, they have been established as important to repolarizing action potentials in several high frequency firing cell types, including those in the auditory system [14,42,50,67]. In this regard, the ELL shares many characteristics with the dorsal cochlear nucleus [33], and can discharge spikes at rates of up to 475 Hz [25]. We therefore initiated a study to clone and sequence the *Shaw* family of K$^+$ channels from a cDNA library established from *Apteronotus* brain. This work has identified two Kv3 genes and obtained partial cDNAs for three other Kv3 genes [44,46,47]. In situ hybridization studies revealed that the apteronotid homologue of Kv3.3, *Apt*Kv3.3, is expressed at very high density in both pyramidal and granule cells of the ELL (Fig. 6A) [46]. Further development of a polyclonal antibody to the C-terminus of *Apt*Kv3.3 revealed that these channels are distributed at apparently high density over the entire soma-dendritic axis of pyramidal cells (Fig. 6B). Indeed, immunolabel was detected over the soma and dendritic processes of the majority of ELL cell types, including granule cells (Fig. 6C), deep basilar pyramidal cells (Fig. 6D), and multipolar cells (Fig. 6D). By com-

parison, double labeling with an antibody to neurofilament revealed little if any *Apt*Kv3.3 immunolabel on axonal membranes or in presynaptic termination zones [45]. The prominence of a dendritic distribution of *Apt*Kv3.3 channels stands in stark contrast to the distribution of any other Kv3 channel subtype, in that Kv3.1, 3.2 and 3.4 channels have been localized only to somatic, axonal or presynaptic membranes [38,53,69,70]. In fact, only a handful of voltage-dependent K$^+$ channels have been localized to dendritic membranes, implying an important role for this channel in signal processing in the ELL.

3.6. Physiological studies of Apt*Kv3.3 K$^+$ channels*

To examine the properties of *Apt*Kv3.3 channels through patch clamp recordings, we developed a novel technique to partially dissociate thin ELL tissue slices to remove a heavy investment of glia in the pyramidal cell body region [46]. The approach of "spread printing" we have used represents an extension of an earlier methodology of tissue printing developed for this system [23],
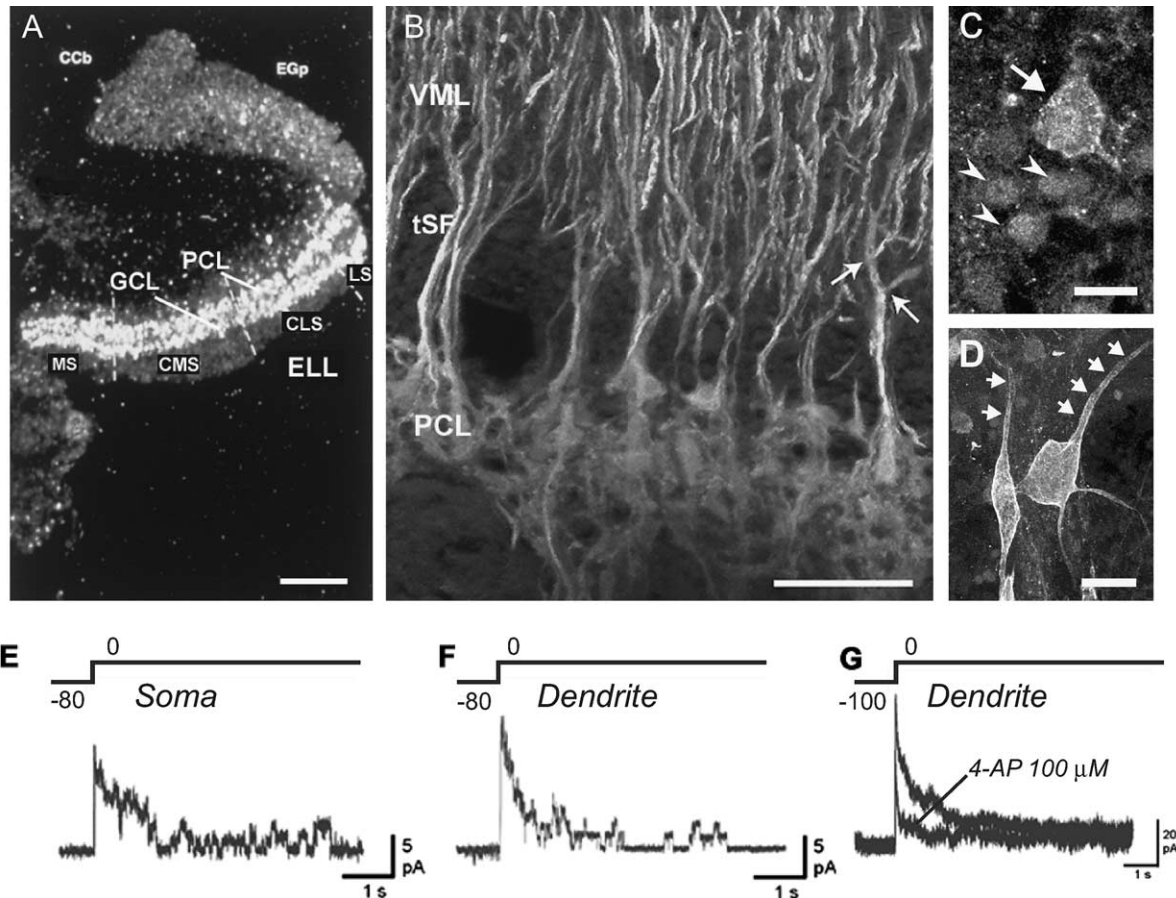
Fig. 6. *Apt*Kv3.3 K$^+$ channels are highly expressed in ELL pyramidal cells. (A) Dark field micrograph indicating distribution of *Apt*Kv3.3 mRNA at the medullary level. Note the dense labeling of the ELL pyramidal (PCL) and granule cell (GCL) body layers. (B) Immunolabel for *Apt*Kv3.3 K$^+$ channels reveals an extensive distribution over the entire soma-dendritic axis of pyramidal cells. *Arrows* indicate labeling past primary and secondary branchpoints. (C) and (D) *Apt*Kv3.3 immunolabel is membrane-associated and distributed over the soma and dendrites of several ELL cell types: granule cell I, *large arrow*; granule cell II, *arrowheads*; deep basilar pyramidal and multipolar cell, *small arrows*. (E) and (F) Outside-out patch clamp recordings obtained from the soma (E) or proximal apical dendrites (F) reveal a high density of fast activating, inactivating K$^+$ channels consistent with Kv3.3 channel kinetics. (G) Low concentrations of 4-AP block *Apt*Kv3 channels, shown here for a dendritic outside-out macropatch recording. Abbreviations not in text: *CCb*, corpus cerebelli; *EGp*, eminentia granularis pars posterior; *VML*, ventral molecular layer. Scale bars represent 500 μm in A, 100 μm in B, 10 μm in C and D. Data are taken from [45,46], with modifications (©2001 by the Society for Neuroscience).

but with far higher cell yield and structural preservation. The strengths of this procedure are that it allows one to obtain a partially dissociated tissue slice within 15 min of cutting tissue sections on a vibratome without the use of proteolytic enzymes. Moreover, the dissociation is primarily restricted to the pyramidal cell body layer, providing an organotypic distribution of cells on a glass coverslip in which synaptic inputs in the molecular layer remain intact. By using differential interference contrast optics and infrared light transmission, we are able to visually identify pyramidal cells and examine the properties of K$^+$ channels in the soma and proximal apical dendrites using on-cell or outside-out patch recordings.

Patch clamp recording studies revealed a high density of voltage-dependent K$^+$ channels in somatic and dendritic membranes that have kinetic properties consistent with Kv3.3 channels [45]. Specifically, channels isolated in the outside-out patch recording mode have a single channel conductance of ∼25 pS, a high threshold for activation of macro-patch currents (∼−20 mV), and a slow inactivation of $\tau = 330 \pm 87$ ms. The channels are also highly sensitive to external application of 4-AP (<100 μM) and TEA (IC$_{50}$ = 78 μM). These properties are virtually identical to those obtained through similar recordings of *Apt*Kv3.3 channels expressed in isolation after transfection of cDNA in human embryonic kidney (HEK) cells. Although CMS pyramidal cells also express *Apt*Kv3.1 K$^+$ channels, the relative density of mRNA is approximately 50:1 *Apt*Kv3.3: *Apt*Kv3.1, suggesting a more prominent expression of *Apt*Kv3.3 channels [46]. *Apt*Kv3.1 channels also give rise to a non-inactivating current when expressed in HEK cells (AJ Rashid, RJ Dunn, unpublished observations). Therefore, the expression pattern and kinetic and pharmacological properties of K$^+$ channels recorded in situ

provides strong support for their identification as *Apt*Kv3.3 K$^+$ channels.

At this time there are no established specific blockers for Kv3.3 K$^+$ channels. Other voltage-dependent channels are also known to be blocked by low concentrations of TEA or 4-AP, including large conductance Ca^{2+}-activated K$^+$ channels (BK) and K$^+$ channels of the Kv1 (*Shaker*) class. However, we recently established that neither of these channel classes contribute to spike repolarization in dendritic or somatic regions of pyramidal cells [39]. As a result, we can use low concentrations of 4-AP or TEA as relatively selective blockers for Kv3 channels to identify their functional role in spike repolarization and burst discharge. These studies established that Kv3 K$^+$ channels contribute to the repolarization of both somatic and dendritic spikes [46]. This led to the prediction, based on our working hypothesis of the interaction between dendritic and somatic spikes (Fig. 2B), that a reduction in dendritic *Apt*Kv3 conductance should modulate DAP amplitude and thus burst discharge. This was tested by focally ejecting 4-AP or TEA in dendritic regions (Fig. 7). We found that dendritic application of 4-AP or TEA slowed the rate of dendritic spike repolarization; promoting an increase in dendritic spike duration (Fig. 7A–C) and a selective potentiation of the DAP at the soma (Fig. 7D–F). As a result, blocking dendritic Kv3 channels reliably shifted cell output from tonic to burst discharge [46]. This provides the important result that reducing the effectiveness of Kv3 channels in repolarizing dendritic spikes can determine the threshold and occurrence of burst discharge in pyramidal cells.

3.7. Simulations of spike backpropagation and burst discharge

In order to further test hypotheses regarding the ionic control of burst discharge, we recently constructed a detailed compartmental model of a basilar pyramidal cell [13]. The model is comprised of 312 compartments varying in diameter from 0.5 to 11.6 μm and adjusted to produce isopotential compartments no longer than 25 μm. The model currently contains 10 ionic currents, including somatic and dendritic fast activating Na$^+$
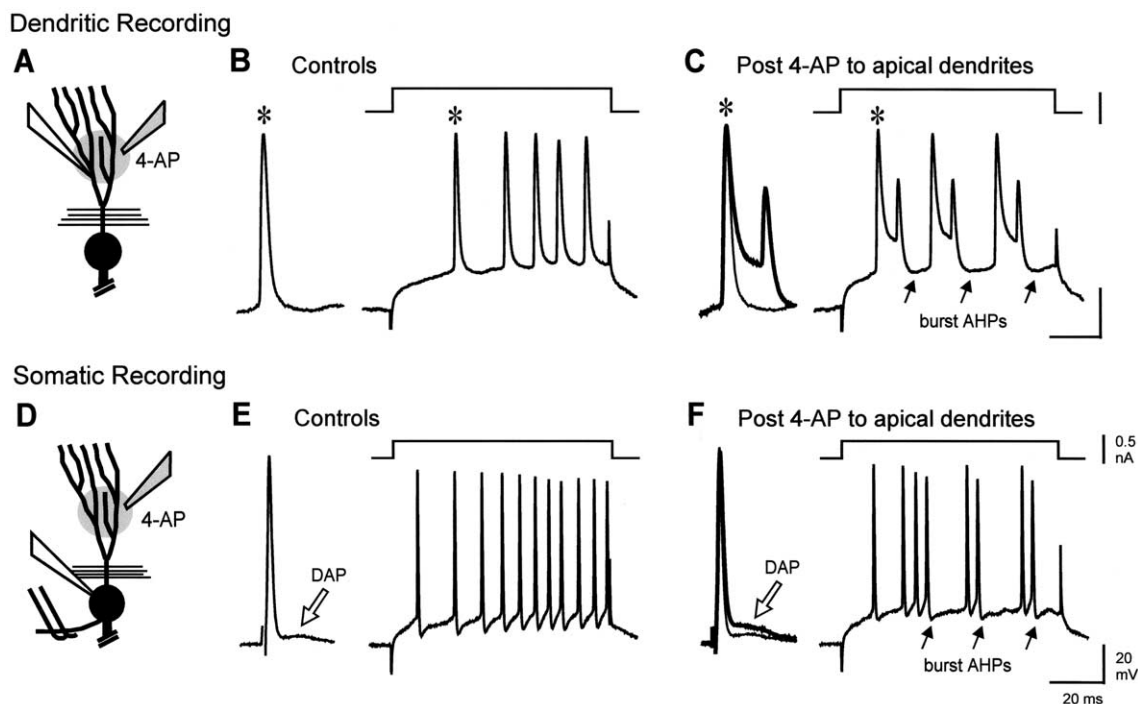

Fig. 7. Dendritic spike repolarization controls burst threshold. (A)–(C) The effects of dendritic 4-AP ejection on dendritic spike discharge. (A), Schematic diagram of a pyramidal cell indicating an intradendritic recording (*white filled electrode*) and pressure electrode for focal ejection of 2 mM 4-AP (*shaded fill*). (B) Control recordings showing current-evoked spike discharge set below threshold for generating burst discharge. *Insets* to the left in B and C show expanded views of the first current-evoked spikes in control and test recordings (*asterisks*). (C) Focal ejection of 4-AP broadens the dendritic spike by slowing spike repolarization and shifts cell output from a tonic to bursting pattern (burst AHPs denoted by *arrows*). *Inset* shows the control and test (*thick trace*) responses superimposed. (D)–(F) The effects of dendritic 4-AP ejection on somatic spike discharge. (D) Schematic diagram of a pyramidal cell indicating an antidromic stimulating electrode (*double wires*), intrasomatic recording electrode (*white fill*), and pressure electrode for focal drug ejection of 2 mM 4-AP (*shaded fill*). (E) Control intrasomatic recordings of antidromic spike discharge and associated DAP (*open arrow*), and current-evoked spike discharge when set below threshold for generating burst discharge. (F) Focal ejection of 4-AP selectively enhances the somatic DAP (*open arrow*) as shown by superimposition of the antidromic control and test (*thick trace*) response. This is sufficient to convert cell output from a tonic to bursting pattern (burst AHPs denoted by *arrows*). Data are taken from [46], with modifications (©2001 by the Society for Neuroscience).

(I_{Na}), fast activating, non-activating persistent Na$^+$ (I_{NaP}), delayed rectifier K$^+$ (I_{Dr}), a fast transient "A"-type K$^+$ current, and *Apt*Kv3.3 K$^+$ channels. The distribution of Na$^+$, NaP, and *Apt*Kv3.3 conductance was guided by immunocytochemical and electrophysiological data [4,25,45,63], and *Apt*Kv3.3 kinetics were matched to those recorded in isolation when expressed in HEK cells [46]. The conductance and distribution of other channels were fit by matching simulations to experimental data of spike discharge properties recorded in vitro.

Fig. 8 illustrates the accuracy of the current model in reproducing somatic spike discharge and backpropagation of spikes over the initial ∼200 μm of apical dendrites (cf Fig. 8A and B). A large difference in the duration of somatic and dendritic spikes leads to the reexcitation of somatic membrane by current flow from dendrite to soma in the form of a DAP. The role of dendritic spikes in DAP generation is evident when removal of active dendritic sites produces a much larger fAHP at the soma (Fig. 8C). The dendritic compartment under these conditions is only excited by a small pre-potential that reflects a passively conducted representation of the somatic spike (Fig. 8C). This agrees with earlier experimental work in which focal dendritic TTX application uncovered a small pre-potential in dendrites that was linked to somatic spike discharge [63]. Finally, the model reproduces an increase in refractory period from soma and over the apical dendrites (not shown).

Despite having in place a representation of spike discharge, conduction, and refractory period over the soma–dendritic axis, we found that the core model generated only tonic spike discharge at all levels of membrane depolarization (Fig. 9A). We therefore tested several ionic factors known to contribute to burst discharge in other cells, including a slowly activating K$^+$ current, dendritic Na$^+$ channel inactivation, and slowly activating inward current. Although some of these manipulations resulted in burst output, none of them produced the key features of conditional backpropagation found in pyramidal cells. In contrast, we found that introducing a single factor, namely a cumulative inactivation of dendritic K$^+$ conductance, was necessary and sufficient to reproduce virtually all aspects of conditional backpropagation and burst discharge (Fig. 9B and C). This included a frequency-dependent broadening of dendritic spikes and potentiation of the DAP, a decrease in ISI during repetitive discharge, and termination of bursts by a spike doublet that blocked backpropagation and the dendritic depolarization driving the burst (Fig. 9D). The subsequent burst AHP that followed each spike doublet was further capable of promoting recovery of the dendritic K$^+$ conductance and all associated changes during the previous burst (Fig. 9C), such that the process of conditional backpropagation could be activated in an oscillatory fashion. The model further reproduced the presence of a distinct threshold separating tonic and burst discharge during current-evoked depolarizations, as reported earlier for pyramidal cells [25].

3.8. Burst discharge invoked by descending synaptic inputs

In considering the functional relevance of burst discharge to electrosensory processing, it will be important to determine the ability for synaptic inputs to trigger or facilitate the generation of spike bursts. One candidate pathway is the tSF, a fast myelinated descending projection that originates in the nucleus praeemenentialis dorsalis (nPd). Stellate cells in the nPd have been shown to receive input from ELL pyramidal cells and
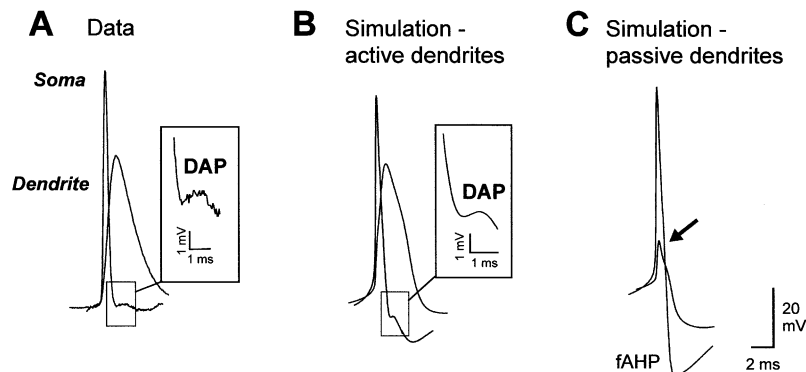

Fig. 8. A compartmental model of pyramidal cell accurately reproduces spike backpropagation. (A), Superimposed antidromically activated spikes from separate somatic and dendritic recordings (∼200 um from soma). Note the difference in spike amplitude and duration between somatic and dendritic sites. The somatic DAP is enlarged in the *inset*. (B), Superimposed somatic and dendritic spike simulations (∼200 μm from the soma) evoked by depolarizing somatic current injection in a compartmental model of pyramidal cells. Note the close correspondence between simulation (B) and experimental data (A). The somatic DAP is enlarged within the *inset* for comparison with A. (C), Superimposed somatic and dendritic spike simulations in the model evoked in response to somatic current injection, but with all Na$^+$ conductance removed from dendritic compartments. Note that the somatic DAP is entirely removed, uncovering a prominent fAHP at the soma. Only a small passive response is reflected into apical dendrites upon the discharge of somatic spikes under this condition (*arrow*). Data are modified from [13] with permission of Journal of Neurophysiology.
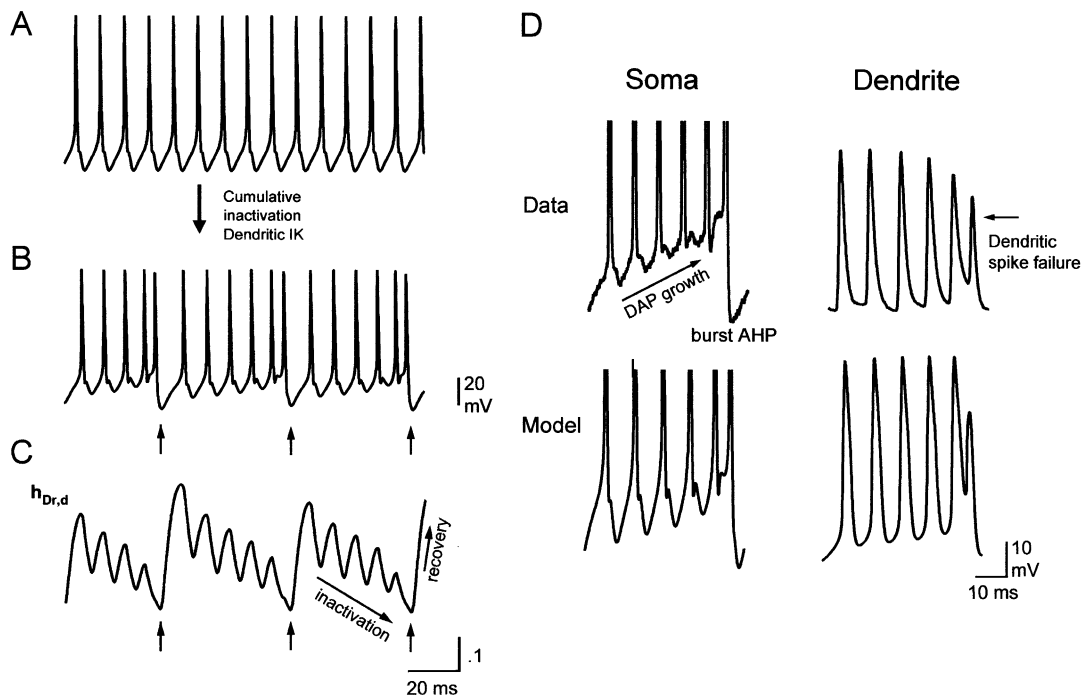
Fig. 9. Cumulative inactivation of dendritic K$^+$ current is sufficient to produce conditional backpropagation and burst discharge. All simulations have a depolarizing current of 0.6 nA applied to the somatic compartment. (A) The core model that reproduces spike backpropagation generates only repetitive spike discharge in response to depolarization (simulations shown at the soma). (B) Introducing a cumulative inactivation of $I_{Dr,d}$ promotes robust burst discharge with all elements inherent to conditional backpropagation; including a gradual decrease in ISI, an increase in DAP amplitude, and the discharge of a spike doublet and subsequent burst AHP. (C) The dynamics of the gating variable $h_{Dr,d}$ as the burst shown in B evolves, indicating a cumulative inactivation of $h_{Dr,d}$ during bursts. Removal of inactivation occurs rapidly during the burst AHP that follows each spike doublet (*arrows*). Units shown correspond to the normalized fraction of open channels. (D) A comparison between experimentally recorded and simulated burst discharge in ELL pyramidal cells. In the top row are expanded traces of somatic and dendritic spike bursts illustrating a DAP potentiation at the soma, dendritic spike broadening, and failure of dendritic backpropagation at the end of spike bursts. In the lower row are comparable views of a single spike burst in the soma and dendrite, as simulated by the compartmental model when a cumulative inactivation of $I_{Dr,d}$ is incorporated. Note the close correspondence in virtually all aspects of spike discharge and afterpotentials between experimental data and simulations. Data are modified from [13] with permission of Journal of Neurophysiology.

topographically project excitatory glutamatergic feedback to the proximal apical dendrites of pyramidal cells [6,51]. This may have particular functional significance, as the site for termination of tSF inputs overlaps closely with the distribution of dendritic Na$^+$ channels that support spike backpropagation [63]. Any reduction of dendritic K$^+$ conductance by synaptic inputs would provide an effective means of recruiting burst discharge according to activity in the ELL–nPd recurrent loop. In fact, focal activation of descending synaptic inputs to the ELL has been proposed by Maler to represent a searchlight mechanism to enhance pyramidal cell activity [5,6].

We have begun to investigate the potential for tSF synaptic inputs to generate burst discharge in pyramidal cells. Bastian et al. [7] established that nPd stellate cells generate spike discharge at frequencies ranging from 25 to 300 Hz during step changes in external electric field strength in vivo. It is interesting that this range falls within that shown to be capable of generating bursts during repetitive spike discharge in pyramidal cells. We have now determined that tSF synaptic inputs can trigger

spike bursts in pyramidal cells in a frequency-dependent fashion (Fig. 10). We found that during dendritic recordings, repetitive activation of the tSF pathway potentiates a subthreshold EPSP to the point of triggering spike discharge within 1–3 stimuli (Fig. 10B). At stimulus intervals above ∼10 ms dendritic spikes evoked during the stimulus train do not change significantly (Fig. 10B). However, if the stimulus interval is reduced below ∼10 ms, each dendritic spike in the stimulus train undergoes a progressive decrease in the rate of repolarization, with a corresponding increase in dendritic spike duration (Fig. 10C; $n=3$). As the interstimulus interval is shortened (i.e. 7 ms) the change in dendritic spike duration proves to be sufficient to eventually block spike backpropagation, as indicated by a dendritic spike doublet (Fig. 10C, arrow). We have not yet determined the full frequency- or voltage-dependence of this effect, but these results are important in revealing the capability of descending synaptic inputs to generate burst discharge by modifying dendritic spike properties.
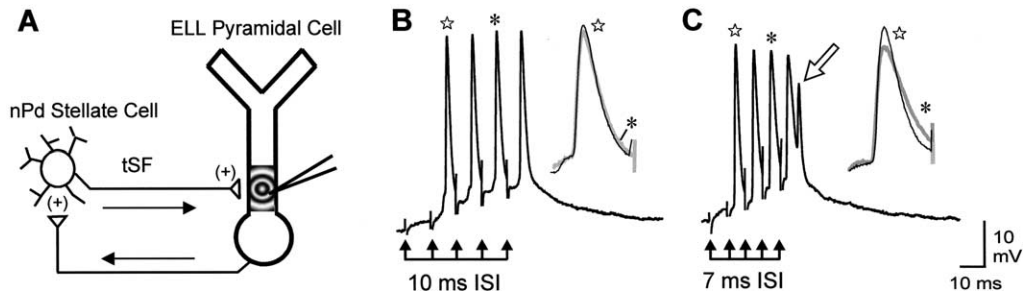
Fig. 10. Descending synaptic inputs evoke burst discharge through a frequency-dependent process. (A) Schematic diagram depicting the excitatory recurrent loop between ELL pyramidal cells and nPd stellate cells and a dendritic recording site. Descending tSF synaptic inputs terminate over the same region as Na^+ channels in pyramidal cell proximal apical dendrites (*circular shading*). (B) and (C) The effects of repetitive stimulation of tSF inputs on the evoked EPSP, spike and burst discharge. Stimuli are indicated by linked arrows and *insets* to the right show expanded and superimposed views of the first (*star, dark trace*) and third spike (*asterisk, grey trace*) in the stimulus trains. Stimulus artifacts have been removed. Repetitive tSF stimulation at a 10 ms interval (B) potentiates the dendritic EPSP but does not change spike properties. In contrast, tSF stimulation at a 7 ms interval (C) leads to dendritic spike broadening (see *inset*) as well as burst discharge, as indicated by the presence of a spike doublet (*open arrow*).

4. Discussion

Our data indicates that ELL pyramidal cells produce burst discharge over a wide range of frequencies through a mechanism not previously recognized in any other bursting cell type. Unlike most bursting cells, there is no apparent involvement of the more classical ion conductances (i.e. I_h, I_T) that produce subthreshold oscillations in membrane potential to generate burst output. Rather, conditional backpropagation depends only on differences in basic parameters of Na^+ spike discharge between somatic and dendritic locations. The simple nature of this process generates a highly reliable series of events in which spike backpropagation is eliminated if cell discharge exceeds the dendritic refractory period. Nevertheless, this mechanism is capable of producing burst output between 5 and 150 Hz; a capability that would be advantageous to a sensory neuron using burst discharge to signify the occurrence of specific events in afferent input. It will thus be important to determine when conditional backpropagation is used to trigger burst discharge in vivo, and how it can be modulated to respond appropriately to changing sensory input.

Notably, the detailed compartmental model presented here was comprised of >1500 differential equations. Yet, recent work indicates that conditional backpropagation can be generated by a reduced model relying on only six differential equations, illustrating the simplicity of the underlying mechanism [12]. Moreover, it becomes clear through use of dynamical systems and bifurcation theory (not possible with the large compartmental model), that generating burst discharge through conditional backpropagation represents a mechanism not recognized in all existing computational burst classification schemes [20].

4.1. Dendritic modulation of cell excitability

A role for backpropagating spikes in producing a DAP at the soma has been suggested for other cell types [16,17,24,30,72,73]. However, this typically involves the activation of dendritic Ca^{2+} currents by a backpropagating Na^+ spike; either through focal blockade of dendritic K^+ currents or by coincident activation of synaptic inputs. We have shown that spike discharge can be grouped into bursts entirely by modulating dendritic Na^+ spikes [13,25]. The decrease in dendritic spike repolarization that leads to conditional backpropagation can be evoked during current injection but also by descending synaptic inputs.

It should be noted that the ISI range of 3–8 ms (125–300 Hz) identified near burst threshold in vitro is lower than the usual rate of $\sim$20 ms (50 Hz) discharge reported for pyramidal cells in vivo, at least during spontaneous activity [3]. However, during evoked responses, published records would indicate spike discharge occurring at intervals in the order of 7 ms [15]. The ISI values identified in vitro at burst threshold must be taken as representative of those required under the relatively hyperpolarized condition of cells maintained in vitro. We have also determined that the ISI required to evoke burst discharge depends on the degree of temporal summation of dendritic spikes, and is therefore subject to regulation according to the rate of preceding spike activity [25]. Recent measurements of ISIs during the presentation of long depolarizations in vitro indicate a transition from tonic to burst discharge at ISIs of up to 11 ms (L. Noonan, R.W. Turner, B. Doiron, unpublished observations). We thus expect that even longer ISIs will be capable of generating burst output in vivo when the additional effects of background synaptic depolarizations and associated change in dendritic conductance come into play.

A second means for dendrites to modulate burst output relates to cell structure and the extent of active dendritic conductances. Modeling studies indicate that the ability for dendritic Na^+ conductance to produce a DAP increases with the ratio of dendritic to somatic surface area [31]. The properties of backpropagating spikes are also highly regulated by the structure of the dendritic arborization [66]. Both of these factors may be very important to burst discharge in the ELL, as Bastian et al. have reported a strong correlation between the length of pyramidal cell apical dendrites and the propensity to generate burst discharge in vivo [2,3]. We are uncertain as to the extent to which dendritic structure has affected estimates of burst threshold in vitro, but it may account for why up to 40% of pyramidal cells do not appear capable of generating spike bursts [25].

4.2. Modulation of burst discharge by dendritic K^+ current

Our modeling studies reveal that a cumulative inactivation of dendritic K^+ current is a highly effective means of producing not only the required dendritic spike broadening but virtually all aspects of conditional backpropagation. A cumulative inactivation of K^+ current is a predicted and frequent consequence of channels that exhibit a voltage- and time-dependent inactivation [22,43,48,60]. It is thus significant that we have identified a high density of the slowly inactivating AptKv3.3 channel in dendritic regions, as it represents a current most likely to contribute to frequency-dependent spike broadening. The ability for this current to modulate burst output was also directly demonstrated through focal drug ejections in the dendrites (Fig. 7). Despite this, we found the need to implement cumulative inactivation in the compartmental model through the dendritic current $I_{Dr,d}$ [13]. This was necessary since the high voltage threshold for AptKv3.3 channels prevented this current from producing a sufficient change in dendritic spike repolarization in the model to generate burst output. This may be due to the fact that AptKv3.3 kinetics in the model were based upon those recorded for AptKv3.3 channels expressed in isolation in HEK cells. Although these kinetics are similar to those recorded by patch clamp analysis in dendritic regions, all these recordings were carried out in the outside-out patch recording configuration, which can potentially wash out modulatory factors. In this regard, it was recently shown that the $V_{1/2}$ for Kv3.1 channel activation and inactivation is shifted by up to −20 mV by dephosphorylation [28]. Kv3.1, 3.2 and 3.4 channels are also modulated by PKC and PKA [1,10,11,21,38,49]. It is thus entirely possible that AptKv3.3 channels are differentially modulated between somatic and dendritic locations, which increase the contribution of these channels to burst output.

Resolving this discrepancy between model and experimental work will require further analysis of AptKv3.3 kinetics in the on-cell mode to preserve potential intracellular modulators. Regardless, the ability to reproduce all the factors involved in conditional backpropagation through a single kinetic process (cumulative inactivation) presents a strong case for the occurrence of this phenomenon in intact pyramidal cells. Another possibility that must be remembered is that AptKv3.3 channels represent only one potential contributor to frequency-dependent changes in dendritic spikes. For instance, our most recent work indicates that persistent Na^+ current (I_{NaP}) can significantly enhance dendritic spike broadening and DAP potentiation in a voltage-dependent fashion (B. Doiron, L. Noonan, R.W. Turner, unpublished observations). Future work will likely identify additional ion channels that contribute to frequency-dependent aspects of burst discharge.

4.3. Role of burst discharge in electrosensory processing

Burst discharge has been recorded in vivo during the presentation of a randomly fluctuating external electric field [15,37]. These studies indicated that spike bursts are preferentially generated during up- or down-strokes in the electric field in a manner that was highly consistent with their identification as E- or I-type pyramidal cells. As such, these authors identified feature extraction as one role for burst discharge in pyramidal cells, as has been found in other sensory systems [26]. A recent study of spontaneous activity in pyramidal cells in vivo reported difficulty in finding consistent evidence of the spike pattern and doublet discharge indicative of conditional backpropagation [3]. However, it is difficult to compare in vitro to in vivo data at this point given differences in burst detection methods, and the potential requirement for an appropriate stimulus to increase the probability for conditional backpropagation.

The potential role for burst discharge to be involved in the frequency tuning of pyramidal cells across sensory maps is still a matter of question. We have preliminary data in vitro that establish clear differences in ion channel gradients that increase the ability to generate burst discharge in LS as compared to CMS pyramidal cells (unpublished observations). One study in vivo specifically examined the potential for differences in burst discharge for feature extraction across ELL maps, but could not find convincing evidence [37]. We can only assume that uncovering differences between maps may depend on specific patterns of input that have not been identified or tested at this time. One contributing factor may be the pattern of descending synaptic feedback. It is interesting that tSF inputs are capable of triggering conditional backpropagation (Fig. 10). Moreover, the 7 ms ISI (140 Hz) discharge rate that induced this effect is well within the range found for tSF afferent inputs in vivo [7]. Further support for the influence of synaptic depolarization was

provided in a recent study that reduced the incidence of burst discharge in vivo by blocking AMPA receptors in the dorsal molecular layer [3]. Burst discharge may then be readily evoked by synaptic feedback to enhance activity in focal populations of pyramidal cells, a result that would be consistent with the proposed role for feedback as part of a searchlight mechanism [5,6]. An increase in burst output in response to synaptic feedback could well serve the purpose of shifting pyramidal cells from a mode of stimulus estimation to stimulus detection [15,37,54]. This is an issue that can be carefully examined in the future using a combination of pyramidal cell recordings and the compartmental model after incorporating realistic descending synaptic feedback.

Acknowledgements

References

[1] M. Atzori, D. Lau, E.P. Tansey, A. Chow, A. Ozaita, B. Rudy, C.J. McBain, H2 histamine receptor-phosphorylation of Kv3.2 modulates interneuron fast spiking, Nat. Neurosci. 3 (2000) 791–798.

[2] J. Bastian, J. Courtright, Morphological correlates of pyramidal cell adaptation rate in the electrosensory lateral line lobe of weakly electric fish, J. Comp. Physiol. [A] 168 (1991) 393–407.

[3] J. Bastian, J. Nguyenkim, Dendritic modulation of burst-like firing in sensory neurons, J. Neurophysiol. 85 (2001) 10–22.

[4] N. Berman, R.J. Dunn, L. MalerFunction of NMDA receptors and persistent sodium channels in a feedback pathway of the electrosensory system, J. Neurophysiology 86 (2001) 1612–1621.

[5] N.J. Berman, L. Maler, Neural architecture of the electrosensory lateral line lobe: adaptations for coincidence detection, a sensory searchlight and frequency-dependent adaptive filtering, J. Exp Biol. 202 (1999) 1243–1253.

[6] N.J. Berman, J. Plant, R.W. Turner, L. Maler, Excitatory amino acid receptors at a feedback pathway in the electrosensory system: implications for the searchlight hypothesis, J. Neurophysiol. 78 (1997) 1869–1881.

[7] B. Bratton, J. Bastian, Descending control of electroreception. II. Properties of nucleus praeeminentialis neurons projecting directly to the electrosensory lateral line lobe, J. Neurosci. 10 (1990) 1241–1253.

[8] J.C. Brumberg, L.G. Nowak, D.A. McCormick, Ionic mechanisms underlying repetitive high-frequency burst firing in supragranular cortical neurons, J. Neurosci. 20 (2000) 4829–4843.

[9] W.H. Calvin, G.W. Sypert, Fast and slow pyramidal tract neurons: an intracellular analysis of their contrasting repetitive firing properties in the cat, J. Neurophysiol. 39 (1976) 420–434.

[10] M. Covarrubias, A. Wei, L. Salkoff, T.B. Vyas, Elimination of rapid potassium channel inactivation by phosphorylation of the inactivation gate, Neuron 13 (1994) 1403–1412.

[11] S.D. Critz, B.A. Wible, H.S. Lopez, A.M. Brown, Stable expression and regulation of a rat brain K + channel, J. Neurochem. 60 (1993) 1175–1178.

[12] B. Doiron, C. Laing, A. Longtin, L. MalerGhostbursting: a novel neuronal burst mechanism, J. Computational Neuroscience 12 (2002) 5–25.

[13] B. Doiron, A. Longtin, R.W. Turner, L. Maler, Model of conditional backpropagation in a sensory neuron, J. Neurophysiology 86 (2001) 1523–1545.

[14] A. Erisir, D. Lau, B. Rudy, C.S. Leonard, Function of specific K(+) channels in sustained high-frequency firing of fast-spiking neocortical interneurons, J. Neurophysiol. 82 (1999) 2476–2489.

[15] F. Gabbiani, W. Metzner, R. Wessel, C. Koch, From stimulus encoding to feature extraction in weakly electric fish, Nature 384 (1996) 564–567.

[16] N.L. Golding, H.Y. Jung, T. Mickus, N. Spruston, Dendritic calcium spike initiation and repolarization are controlled by distinct potassium channel subtypes in CA1 pyramidal neurons, J. Neurosci. 19 (1999) 8789–8798.

[17] R. Granit, D. Kernell, R.S. Smith, Delayed depolarization and the repetitive response to intracellular stimulation of mammalian motoneurones, J. Physiol. (Lond.) 168 (1963) 890–910.

[18] C.M. Gray, D.A. McCormick, Chattering cells: superficial pyramidal neurons contributing to the generation of synchronous oscillations in the visual cortex, Science 274 (1996) 109–113.

[19] D.A. Hoffman, J.C. Magee, C.M. Colbert, D. Johnston, K + channel regulation of signal propagation in dendrites of hippocampal pyramidal neurons, Nature 387 (1997) 869–875.

[20] E.M. Izhikevich, Neural excitability, spiking, and bursting, Int. J. Bifurc. Chaos 10 (2000) 1171–1269.

[21] T. Kanemasa, L. Gan, T.M. Perney, L.Y. Wang, L.K. Kaczmarek, Electrophysiological and pharmacological characterization of a mammalian Shaw channel expressed in NIH 3T3 fibroblasts, J. Neurophysiol. 74 (1995) 207–217.

[22] K.G. Klemic, C.C. Shieh, G.E. Kirsch, S.W. Jones, Inactivation of Kv2.1 potassium channels, Biophys. J. 74 (1998) 1779–1789.

[23] S.A. Kotecha, D.W. Eley, R.W. Turner, Tissue printed cells from teleost electrosensory and cerebellar structures, J. Comp. Neurol. 386 (1997) 277–292.

[24] M.E. Larkum, J.J. Zhu, B. Sakmann, A new cellular mechanism for coupling inputs arriving at different cortical layers, Nature 398 (1999) 338–341.

[25] N. Lemon, R.W. Turner, Conditional spike backpropagation generates burst discharge in a sensory neuron, J. Neurophysiol. 89 (2000) 1519–1530.

[26] J.E. Lisman, Bursts as a unit of neural information: making unreliable synapses reliable, Trends Neurosci. 20 (1997) 38–43.

[27] F.S. Lo, R.J. Cork, R.R. Mize, Physiological properties of neurons in the optic layer of the rat's superior colliculus, J. Neurophysiol. 80 (1998) 331–343.

[28] C.M. Macica, L.K. Kaczmarek, Casein kinase 2 determines the voltage dependence of the Kv3.1 channel in auditory neurons and transfected cells, J. Neurosci. 21 (2001) 1160–1168.

[29] J. Magee, D. Hoffman, C. Colbert, D. Johnston, Electrical and calcium signaling in dendrites of hippocampal pyramidal neurons, Ann. Rev. Physiol. 60 (1998) 327–346.

[30] J.C. Magee, M. Carruth, Dendritic voltage-gated ion channels regulate the action potential firing mode of hippocampal CA1 pyramidal neurons, J. Neurophysiol. 82 (1999) 1895–1901.

[31] Z.F. Mainen, T.J. Sejnowski, Influence of dendritic structure on firing pattern in model neocortical neurons, Nature 382 (1996) 363–366.

[32] L. Maler, The posterior lateral line lobe of certain gymnotoid fish: quantitative light microscopy, J. Comp. Neurol. 183 (1979) 323–363.

[33] L. Maler, E. Mugnaini, Comparison between the fish electrosensory lateral line lobe and the mammalian dorsal cochlear nucleus, J. Comp. Physiol. [A] 173 (1993) 683–685.

[34] L. Maler, E.K. Sas, J. Rogers, The cytology of the posterior lateral line lobe of high-frequency weakly electric fish (Gymnoti-

dae): dendritic differentiation and synaptic specificity in a simple cortex, J. Comp. Neurol. 195 (1981) 87–139.

[35] D.A. McCormick, J.R. Huguenard, A model of the electrophysiological properties of thalamocortical relay neurons, J. Neurophysiol. 68 (1992) 1384–1400.

[36] W. Metzner, J. Juranek, A sensory brain map for each behavior? Proc. Natl. Acad. Sci. USA 94 (1997) 14798–14803.

[37] W. Metzner, C. Koch, R. Wessel, F. Gabbiani, Feature extraction by burst-like spike patterns in multiple sensory maps, J. Neurosci. 18 (1998) 2283–2300.

[38] H. Moreno, C. Kentros, E. Bueno, M. Weiser, A. Hernandez, E. Vega-Saenz de Miera, A. Ponce, W. Thornhill, B. Rudy, Thalamocortical projections have a K+ channel that is phosphorylated and modulated by cAMP-dependent protein kinase, J. Neurosci. 15 (1995) 5486–5501.

[39] L.M. Noonan, E. Morales, A.J. Rashid, R.J. Dunn, R.W. Turner, Kv3.3 channels have multiple roles in regulating somatic and dendritic spike discharge, Proc. Soc. Neurosci. 26 (2) (2000) 1638.

[40] C. Pedroarena, R. Llinas, Dendritic calcium conductances generate high-frequency oscillation in thalamocortical neurons, Proc. Natl. Acad. Sci. USA 94 (1997) 724–728.

[41] M. Penttonen, A. Kamondi, L. Acsady, G. Buzsaki, Gamma frequency oscillation in the hippocampus of the rat: intracellular analysis in vivo, Eur. J. Neurosci. 10 (1998) 718–728.

[42] T.M. Perney, L.K. Kaczmarek, Localization of a high threshold potassium channel in the rat cochlear nucleus, J. Comp. Neurol. 386 (1997) 178–202.

[43] E.A. Quattrocki, J. Marshall, L.K. Kaczmarek, A Shab potassium channel contributes to action potential broadening in peptidergic neurons, Neuron 12 (1994) 73–86.

[44] A.J. Rashid, R.J. Dunn, Sequence diversity of voltage-gated potassium channels in an electric fish, Brain Res. Mol. Brain Res. 54 (1998) 101–107.

[45] A.J. Rashid, R.J. Dunn, R.W. Turner, A prominent soma-dendritic distribution of Kv3.3 K+ channels in electrosensory and cerebellar neurons, J. Comparative Neurology 441 (2001) 234–247.

[46] A.J. Rashid, E. Morales, R.W. Turner, R.W. Dunn, The contribution of dendritic Kv3 K+ channels to burst threshold in a sensory neuron, J. Neurosci. 21 (2001) 125–135.

[47] A.J.a.D.R.J. Rashid, Molecular characterization of two Kv3-type K channels in a vertebrate sensory neuron, Int. Proc. Soc. Neurosci. 25 (1999).

[48] J. Roeper, C. Lorra, O. Pongs, Frequency-dependent inactivation of mammalian A-type K+ channel KV1.4 regulated by Ca2+/calmodulin-dependent protein kinase, J. Neurosci. 17 (1997) 3379–3391.

[49] B. Rudy, A. Chow, D. Lau, Y. Amarillo, A. Ozaita, M. Saganich, H. Moreno, M.S. Nadal, R. Hernandez-Pineda, A. Hernandez-Cruz, A. Erisir, C. Leonard, E. Vega-Saenz-de-Miera, Contributions of Kv3 channels to neuronal excitability, Ann. N. Y. Acad. Sci. 868 (1999) 304–343.

[50] B. Rudy, C.J. McBain, Kv3 channels: voltage-gated K+ channels designed for high-frequency repetitive firing, Trends Neurosci. 24 (2001) 517–526.

[51] E. Sas, L. Maler, The nucleus praeeminentialis: a Golgi study of a feedback center in the electrosensory system of gymnotid fish, J. Comp. Neurol. 221 (1983) 127–144.

[52] P. Schwindt, J.A. O'Brien, W. Crill, Quantitative analysis of firing properties of pyramidal neurons from layer 5 of rat sensorimotor cortex, J. Neurophysiol. 77 (1997) 2484–2498.

[53] C. Sekirnjak, M.E. Martone, M. Weiser, T. Deerinck, E. Bueno, B. Rudy, M. Ellisman, Subcellular localization of the K+ channel subunit Kv3.1b in selected rat CNS neurons, Brain Res. 766 (1997) 173–187.

[54] S.M. Sherman, Tonic and burst firing: dual modes of thalamocortical relay, Trends Neurosci. 24 (2001) 122–126.

[55] C.A. Shumway, Multiple electrosensory maps in the medulla of weakly electric gymnotiform fish. I. Physiological differences, J. Neurosci. 9 (1989) 4388–4399.

[56] N. Spruston, Y. Schiller, G. Stuart, B. Sakmann, Activity-dependent action potential invasion and calcium influx into hippocampal CA1 dendrites, Science 268 (1995) 297–300.

[57] M. Steriade, R. Curro-Dossi, D. Contreras, Electrophysiological properties of ntralaminar thalamocortical cells discharging rhythmic (approximately 40 HZ) spike-bursts at approximately 1000 HZ during waking and rapid eye movement sleep, Neuroscience 56 (1993) 1–9.

[58] M. Steriade, D.A. McCormick, T.J. Sejnowski, Thalamocortical oscillations in the sleeping and aroused brain, Science 262 (1993) 679–685.

[59] M. Steriade, I. Timofeev, N. Durmuller, F. Grenier, Dynamic properties of corticothalamic neurons and local cortical interneurons generating fast rhythmic (30-40 Hz) spike bursts, J. Neurophysiol. 79 (1998) 483–490.

[60] J.F. Storm, Temporal integration by a slowly inactivating K+ current in hippocampal neurons, Nature 336 (1988) 379–381.

[61] G. Stuart, N. Spruston, B. Sakmann, M. Hausser, Action potential initiation and backpropagation in neurons of the mammalian CNS, Trends Neurosci. 20 (1997) 125–131.

[62] R.D. Traub, N. Spruston, I. Soltesz, A. Konnerth, M.A. Whittington, G.R. Jefferys, Gamma-frequency oscillations: a neuronal population phenomenon, regulated by synaptic and intrinsic cellular processes, and inducing synaptic plasticity, Prog. Neurobiol. 55 (1998) 563–575.

[63] R.W. Turner, L. Maler, T. Deerinck, S.R. Levinson, M.H. Ellisman, TTX-sensitive dendritic sodium channels underlie oscillatory discharge in a vertebrate sensory neuron, J. Neurosci. 14 (1994) 6453–6471.

[64] R.W. Turner, D.E. Meyers, T.L. Richardson, J.L. Barker, The site for initiation of action potential discharge over the somato-dendritic axis of rat hippocampal CA1 pyramidal neurons, J. Neurosci. 11 (1991) 2270–2280.

[65] R.W. Turner, J.R. Plant, L. Maler, Oscillatory and burst discharge across electrosensory topographic maps, J. Neurophysiol. 76 (1996) 2364–2382.

[66] P. Vetter, A. Roth, M. Hausser, Propagation of action potentials in dendrites depends on dendritic morphology, J. Neurophysiol. 85 (2001) 926–937.

[67] L.Y. Wang, L. Gan, I.D. Forsythe, L.K. Kaczmarek, Contribution of the Kv3.1 potassium channel to high-frequency firing in mouse auditory neurones, J. Physiol. (Lond.) 509 (1998) 183–194.

[68] X.J. Wang, Fast burst firing and short-term synaptic plasticity: a model of neocortical chattering neurons, Neuroscience 89 (1999) 347–362.

[69] M. Weiser, E. Bueno, C. Sekirnjak, M.E. Martone, H. Baker, D. Hillman, S. Chen, W. Thornhill, M. Ellisman, B. Rudy, The potassium channel subunit KV3.1b is localized to somatic and axonal membranes of specific populations of CNS neurons, J. Neurosci. 15 (1995) 4298–4314.

[70] M. Weiser, E. Vega-Saenz-de-Miera, C. Kentros, H. Moreno, L. Franzen, D. Hillman, H. Baker, B. Rudy, Differential expression of Shaw-related K+ channels in the rat central nervous system, J. Neurosci. 14 (1994) 949–972.

[71] S.R. Williams, G.J. Stuart, Action potential backpropagation and somato-dendritic distribution of ion channels in thalamocortical neurons, J. Neurosci. 20 (2000) 1307–1317.

[72] R. Yuste, M.J. Gutnick, D. Saar, K.R. Delaney, D.W. Tank, Ca2+ accumulations in dendrites of neocortical pyramidal neurons: an apical band and evidence for two functional compartments, Neuron 13 (1994) 23–43.

[73] L. Zhang, T.A. Valiante, P.L. Carlen, Contribution of the low-threshold T-type calcium current in generating the post-spike depolarizing afterpotential in dentate granule neurons of immature rats, J. Neurophysiol. 70 (1993) 223–231.